Comparison of Speed Control Strategies for Maximum Power Tracking in a Wind Energy Conversion System

J. Zaragoza[1], C. Spiteri Staines[2], A. Arias[1], J. Pou[1], E. Robles[3], S. Ceballos[3]

[1] *Electronic Engineering Dept. Technical University of Catalonia. Campus Terrassa. C. Colom 1. 08222 Terrassa. Catalunya. Spain.*
zaragoza@eel.upc.edu, arias@eel.upc.edu, *pou@eel.upc.edu*

[2] *Department of Industrial Electrical Power Conversion, University of Malta. Faculty of Engineering. Msida, Malta*
[2]cjspit@eng.um.edu.mt

[3]*Energy Unit. Robotiker-Tecnalia Technology Corporation. Zamudio, Basque Country, Spain*
erobles@robotiker.es, sceballos@robotiker.es

***Abstract*—This paper presents two different variable-speed control strategies to obtain the maximum power from wind turbines (WT). The two control strategies are composed by three regulators, which may be based on linear or nonlinear controllers. The first control strategy is composed of three standard proportional-integral (PI) regulators. The PI controllers are tuned for a specific operation mode. However, since the system is nonlinear, for different operating conditions, the values of the PI parameters may not be optimal. The second control approach includes a nonlinear (fuzzy) controller to compensate for the nonlinearity of the WT, to achieve improved speed performance under different operating points. The proposed control strategy uses a fuzzy controller and two standard PIs. The results show that in most cases the fuzzy controller obtains superior performance to that of the standard PI-based solution.**

I. INTRODUCTION

Nowadays, the use of the variable speed wind turbines is becoming more and more common for several reasons such as: better capture of wind energy, reduction of mechanical stress, and acoustic noise reduction from blades movement. Fig. 1 shows one type of variable speed WT system based on a permanent-magnet synchronous generator (PMSG). This structure makes use of two back-to-back-connected power converters [1]-[5]. In this configuration, one converter controls the speed of the WT, whilst the other one takes care of shaping the currents injected into the electrical grid. In this set-up, the active and reactive power can be controlled independently.

Using a PMSG: very high torque can be achieved at low speeds; no significant losses are generated in the rotor; lower operational noise is achieved; and external excitation current is not needed [6]-[8]. For all these reasons, it is expected that the PMSG will be extensively used in the future. This paper is devoted to the study of the variable speed control of the PMSG in order to improve its performance in WT systems.

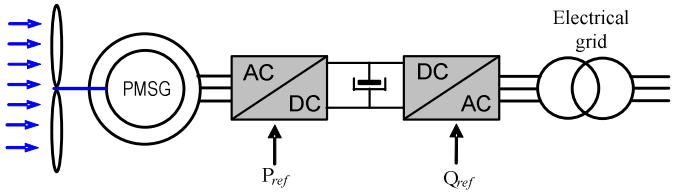

Fig. 1. Variable wind speed systems.

In this work, Field-Oriented Control (FOC) [9], [10] of the PMSG is implemented to achieve variable speed. Two types of controllers have been tested for the outer speed loop; a linear and a nonlinear controller.

In a WT system, the electrical system can be assumed to behave in a linear way. However, due to the aerodynamics, the mechanical system behaves in a nonlinear way; hence, the complete WT system can globally be considered to be nonlinear.

To improve the performance of the WT under varying operating conditions, a nonlinear controller based on fuzzy techniques is proposed in this work. The overall system performance is compared with linear control based on standard PI regulators.

II. WT MODELING

The mechanical power (P_T), can be given by the following equation:

$$P_T = \frac{1}{2}\rho A C_p(\lambda,\beta) v_{wind}^3 , \quad (1)$$

where ρ is the air density (Kg/m^3) which normally takes values in the range [1.22,1.3], A is the area swept by the turbine blades (m^2), and v_{wind} is the wind speed (m/s). The

coefficient C_p relates the kinetic wind energy to the mechanical power. This coefficient depends on two parameters; β which is the blade pitch angle, and λ which is the tip speed ratio defined as follows:

$$\lambda = \frac{\Omega R}{v_{wind}}, \tag{2}$$

where Ω is the angular shaft speed (rad/s) and R is the blade radius (m).

The power coefficient $C_p(\lambda,\beta)$ is nonlinear and depends on the blades aerodynamic design and operating conditions. For this reason, it is difficult to model. Consequently, a generic equation is normally used for the model $C_p(\lambda,\beta)$ [11]-[13]:

$$C_p(\lambda,\beta) = c_1\left(\frac{c_2}{\lambda_i} - c_3\beta - c_4\right)e^{-\frac{c_5}{\lambda_i}} + c_6\lambda, \tag{3}$$

with $\frac{1}{\lambda_i} = \frac{1}{\lambda + 0.08\beta} - \frac{0.035}{\beta^3 + 1}$.

The coefficients c_1 to c_6 depend on the blades shape and its aerodynamic performance.

Equations (2) and (3) are used to implement the wind turbine model. The mechanical torque (T_m) is given by:

$$T_m = \frac{P_T}{\Omega}, \tag{4}$$

Fig. 2 shows C_p curves for different constant values of β. In these representations, the values of the coefficients c_1 to c_6 were taken as: c_1=0.5176, c_2=116, c_3=0.4, c_4=5, c_5=21 and c_6=0.0068, [11]-[13]. Operation at maximum power occurs at β=0º and λ=8.1. This value of tip-speed ratio, $\lambda=\lambda_{opt}$=8.1 (Fig. 2), yields a power coefficient of C_{pmax}=0.48 is achieved for a value of Thus, the optimal angular speed, from (2), and the maximum mechanical power, from (1), are given by:

$$\Omega_{opt} = \frac{\lambda_{opt} v_{wind}}{R} \quad \text{and} \tag{5}$$

$$P_{T\max} = \frac{1}{2}\rho A C_{p\max} v_{wind}^3. \tag{6}$$

For maximum mechanical power operation (P_{Tmax}), the pitch angle is kept constant at β=0º and the optimal speed value ($\Omega^*=\Omega_{opt}$) is provided as reference to the controller.

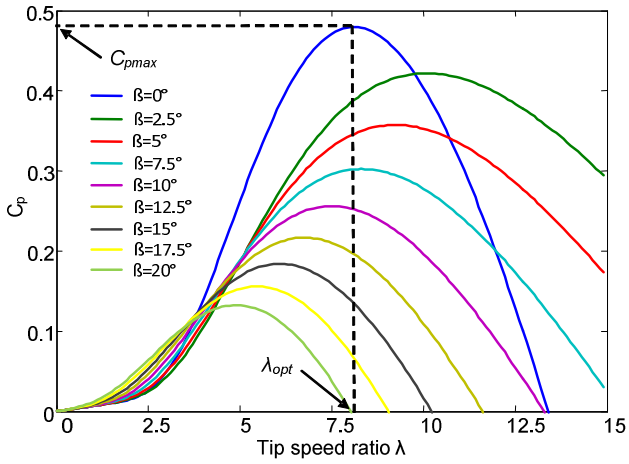

Fig. 2. Power coefficient *Cp* for constant values of β.

Variable speed operation of the WT takes place for a range of wind speeds starting from a lower limit ($v_{\min}$) up to higher wind speeds. For wind speeds below the minimum value, the wind turbine does not operate since the low wind energy present is not enough to compensate for losses and operation costs. On the other hand, at higher wind speeds, the WT control is based solely on pitch angle control.

In this work, the control strategy is focused on variable speed and fixed pitch angle [14] as is commonly used in commercial WT operating under low and medium wind speeds.

III. PMSG Modeling

The parameters of the WT system and the PMSG used in this work are shown in Table I. This PMSM is modeled in the rotating d-q reference frame as follows:

$$v_d = R_s i_d + L_d \frac{d}{dt} i_d - \omega_e L_q i_q \quad \text{and} \tag{7}$$

$$v_q = R_s i_q + L_q \frac{d}{dt} i_q + \omega_e L_d i_d + \omega_e \Psi_m, \tag{8}$$

where v_d and v_q are the stator voltages (V); i_d and i_q are the stator currents (A); R_s is the stator resistance (Ω) of the winding; L_d and L_q are the inductances (mH); ω_e the electrical speed (rad/s); and Ψ_m is the magnetic flux (Wb).

The electrical torque (T_e) is determined by:

$$T_e = \frac{3}{2} p\left[\Psi_m i_q + \left(L_d - L_{sq}\right) i_d i_q\right], \tag{9}$$

where p are the pair of poles.

The rotor dynamics is described by:

$$T_e = T_m + B\omega_r + J\frac{d\omega_r}{dt}, \tag{10}$$

where B is the rotational friction (kg·m^2/s); J is the rotational inertia (kg·m^2); and ω_r the rotational speed (rad/s).

The PMSM FOC diagram shown in Fig. 3 has two control loops:

1. An external mechanical loop, which is responsible for the speed regulation, and

2. two inner current loops, which adjust the generator currents (i_d and i_q).

The optimal speed calculated according to the point of operation is provided as a reference to the external speed loop ($\omega_r^* = \Omega_{opt}$), which generates the quadrature current reference (i_q^*). The outputs of the current loops are the power converter's voltage demand (v_d and v_q).

The current loops are not critical because their dynamic is determined by the system's electrical characteristics which is relatively fast compared to mechanical system's dynamics. Therefore, standard PI controllers can be used to regulate the PMSM's current. However, the external speed loop's dynamic is slow and, additionally, the mechanical system is nonlinear. For these reasons, this is a critical control loop. Two types of regulators are tested for the external loop; a standard PI and a Fuzzy controller.

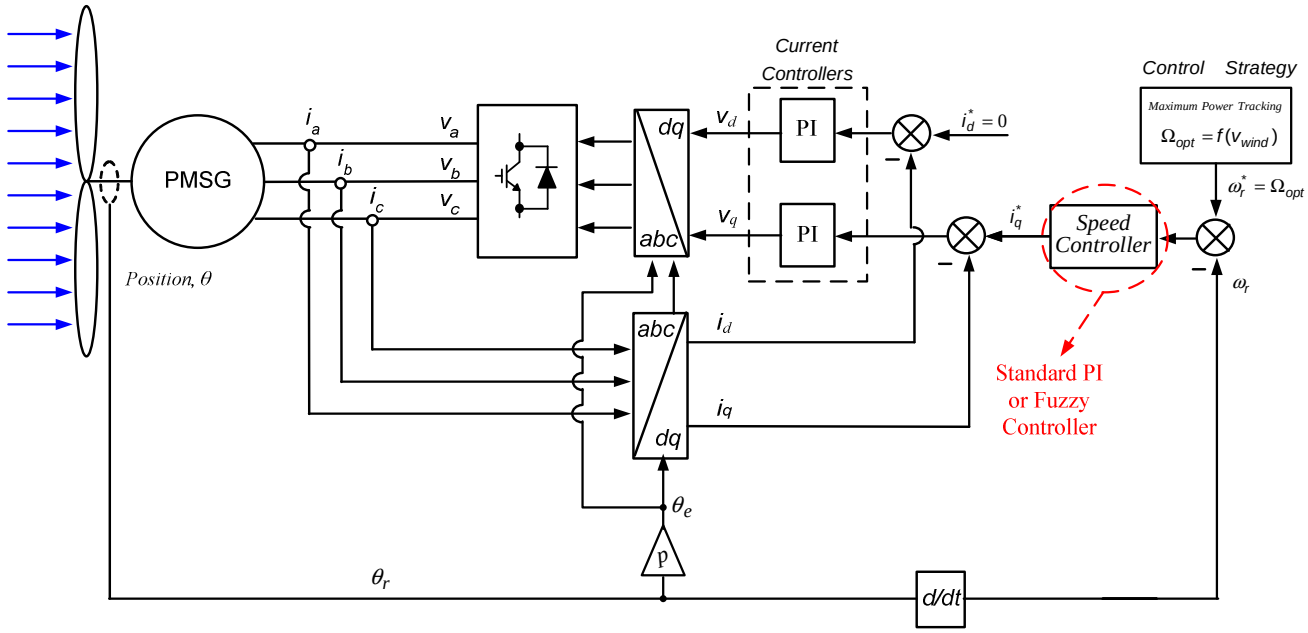

Fig. 3. FOC applied to the wind turbine system.

The electrical and mechanical plants can be simplified to first-order transfer functions, as follows:

$$G_1(s) = \frac{1}{Ls + R_s} \tag{12}$$

$$G_2(s) = \frac{1}{Js + B} \tag{13}$$

The PI controller is mathematically represented by:

$$G_C(s) = k_p + \frac{k_i}{s} = k_i \frac{1 + \frac{k_p}{k_i} s}{s}. \tag{14}$$

The closed-loop transfer functions are as follows:

$$G_{1\_cl}(s) = \frac{\frac{k_i}{L}\left(\frac{k_p}{k_i} s + 1\right)}{s^2 + s\left(\frac{k_p + R_s}{L}\right) + \frac{k_i}{L}} \tag{15}$$

$$G_{2\_cl}(s) = \frac{\frac{k_i}{J}\left(\frac{k_p}{k_i} s + 1\right)}{s^2 + s\left(\frac{k_p + B}{J}\right) + \frac{k_i}{J}} \tag{16}$$

In order to improve the control bandwidth, a pre-filter $G_f(s)$ can be used for all the control loops. This pre-filter is designed to cancel out the zero of the closed-loop transfer function by the following expression:

$$G_f(s) = \frac{1}{\frac{k_p}{k_i} s + 1} \tag{17}$$

The parameters k_p and k_i of the PI controllers are found by defining a rise time (T_r) and damping factor (D_f). In the case of the speed loop, the rise time is around one second and a damping factor of 0.707 is selected. Fig. 4 shows the different speed step responses with and without a pre-filter. These results show a marked improvement when using the pre-filter.

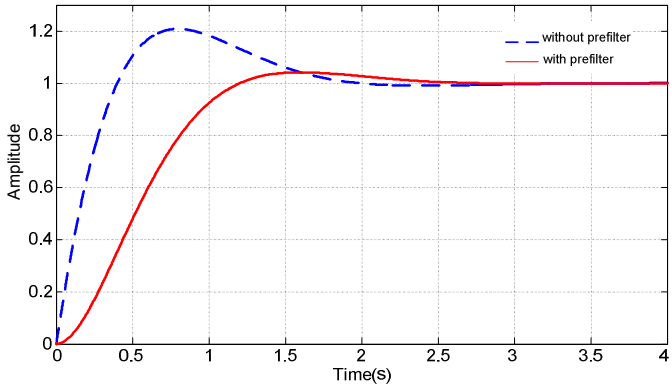

Fig. 4. Step response with and without pre-filter.

TABLE I
DATA OF THE SYSTEM

PMSG	Value	Turbine	Value
P_N(kW)	13.5	Radius blade (m)	5.18
w_N (rpm)	120	Current loop_PI	Value
T_m (Nm)	1,074	k_i	5,940
Rated voltage (V)	400	k_p	13.07
Pole pairs (ρ)	10	Speed loop_PI	Value
L (mH)	16.416	k_i	1,586.6
J (kg·m^2)	206.5	k_p	809.166
B (kg·m^2/s)	1.5		
R_s (Ω)	0.686		

IV. Fuzzy-PI's Controller

In order to improve the outer speed loop response, under all operating conditions, a fuzzy logic controller was designed for this loop. As discussed, standard PI controllers are suitable for the current controllers and were implemented for these loops.

The PID-Fuzzy control structure [15]-[17] uses two input variables and provides one output variable. The input variables are the speed error and its the derivative, like in a conventional PD controller. As the output signal goes through an integrator, the resulting characteristic is similar to a PID controller.

The PID-Fuzzy is suited to the zero-order Takagi-Sugeno fuzzy architecture [17], [18], which is biunivocally described by a set of IF-THEN rules such as:

$$\text{if } x_1 \text{ is } \tilde{x}_{1i} \text{ and ... and } x_n \text{ is } \tilde{x}_{ni} \text{ then } u_i = C_i, \quad (18)$$

where $x_1,..x_n$ are the physical inputs to the fuzzy supervisor. The rule antecedents (part IF of the rule) $\tilde{x}_{1i},...\tilde{x}_{ni}$ are variables described by means of membership functions (Fig. 5), which are in charge of locally and gradually map the corresponding physical variables into the [0, 1] interval.

The rule consequents (part THEN of the rule) are defined as singletons (i.e. $u_i=C_i$, where C_i is the degree of change of the controller parameters), shown in Table II. The inference result of each rule consists of the logic-product of factor ω_i and C_i. The factor ω_i is obtained by applying the min operation on the $\mu_e(e_o)$ and $\mu ce(ce_o)$ as follows:

$$\omega_i = \min\{\mu_e(e_o), \mu_{ce}(ce_o)\}, \quad (19)$$

in which the variables e_o and ce_o are the singleton inputs, where e is the speed error (noted as $e= \omega_r^* - \omega_r$) and ce is its derivative.

Finally, the output of the fuzzy controller u is given by the method of center of gravity, as follows:

$$u = \sum_{i=1}^{N} \omega_i C_i \Big/ \sum_{i=1}^{N} \omega_i , \quad (20)$$

where N is the maximum number of effective rules. In this case, N=4.

The integral action restores the value of the fuzzy controller coefficient u_i, in accordance with:

$$u_i = k(n) = k(n-1) + \Delta k(n) . \quad (21)$$

Fig. 6 shows the three dimensional control surface (two inputs and one output) resulting from this controller. It can be observed that the control actuation is smooth for small speed errors and large for large error values. Consequently, this control strategy will provide some advantages compared to the standard PI controller because the control actuation is adjusted to the situation (nonlinear controller).

The main objective of this surface is to apply different control actions to obtain a desirable performance. The control surface proposed in this work was defined to perform well under different disturbances and wind speeds.

TABLE II
Rule Table of the Fuzzy Controller

e_o\ ce_o	NB	NS	Z	PS	PB
PB	-0.3	-0.35	-0.45	-0.65	-1
PS	0	-0.1	-0.2	-0.35	-0.5
Z	0.2	0.1	0	-0.1	-0.2
NS	0.5	0.35	0.2	0.1	0
NB	1	0.65	0.45	0.35	0.3

V. Simulation Results

The complete WT system was simulated by Simulink using the parameters given in Table I. Fig. 7 shows speed control of the WT system for both types of controllers tested.

The figure compares the transient performance of the PI-based controller and the proposed Fuzzy controller.

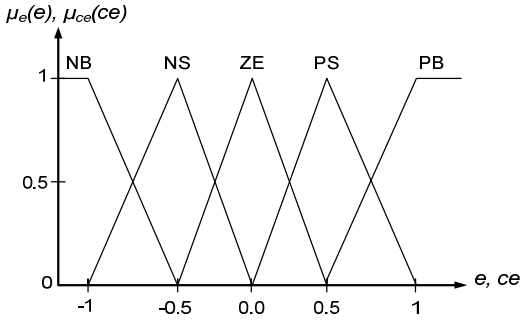

Fig. 5. Membership functions for e and ce.

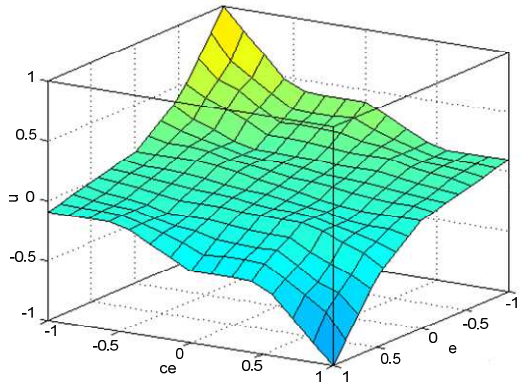

Fig. 6. Resulting input-output supervisor surface.

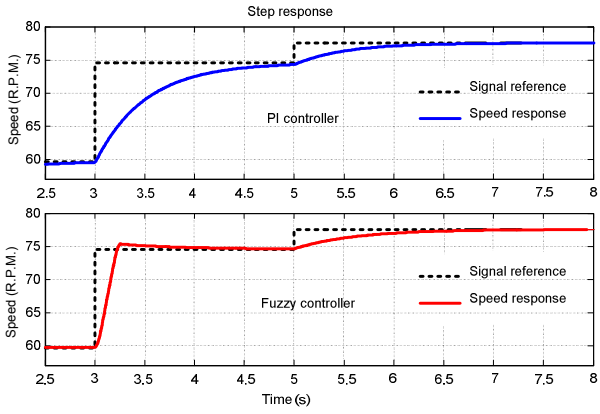

Fig. 7. Speed operation under speed changes.

The simulations show that for small changes in speed demand, similar responses are obtained for both types of controllers. On the other hand, as expected, for large speed reference changes, the fuzzy controller obtains a better response (due to the control surface of Fig. 6 used to tune the fuzzy controller to respond rapidly to large speed errors).

Fig. 8 and Fig. 9 show several waveforms of the simulation wind energy conversion system (WECS) using a wind model development by RISØ National Laboratory [19]. For these simulations, a low average wind speed with a turbulence intensity of 10%, and sample time of 0.05 s was assumed.

Fig. 8 and 9 show the variation of the performance coefficient (C_p), the optimal and real rotor speeds (ω^*_r and ω_r, respectively), and the mechanical torque (T_m). In Fig. 8, a high torque disturbance has been added to the mechanical torque with a standard PI speed controller. This disturbance produces a high overshoot in the speed and a decrease of the C_p coefficient. Furthermore, this coefficient also decreases due to rotational turbulences. Unlike Fig. 8, these unwanted responses are not observed in Fig. 9 operating under the fuzzy controller.

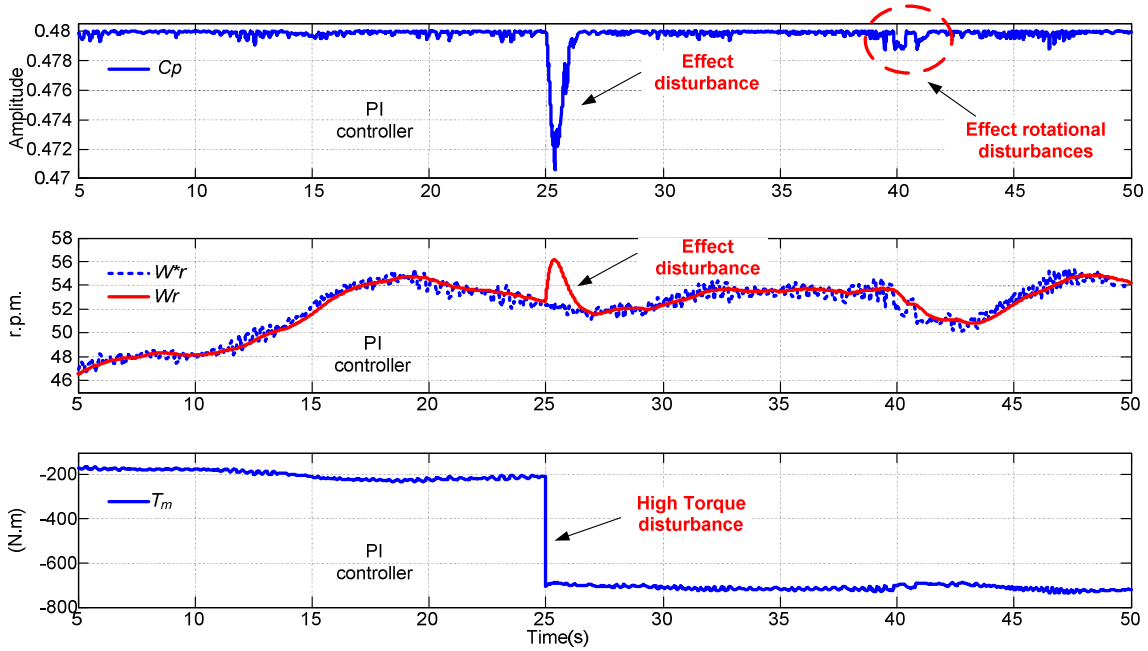

Fig. 8. PI controller performance. (a) Power Coefficient, C_p; (b) rotor speed, w_r; and (c) Mechanical torque, T_m.

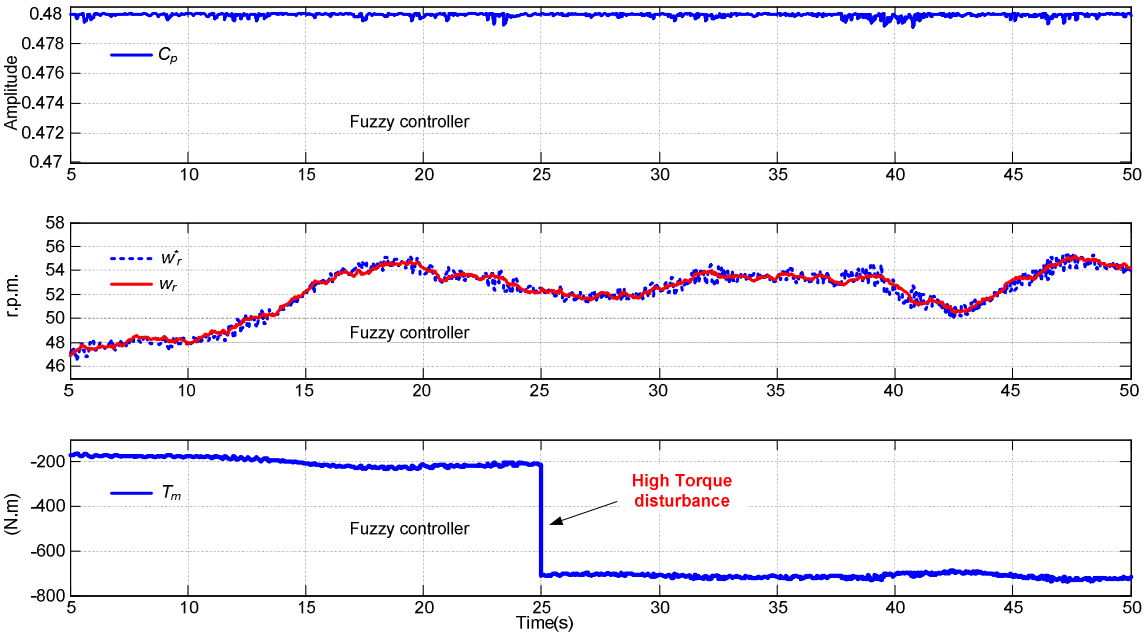

Fig. 9. Fuzzy controller performance. (a) Power Coefficient, C_p; (b) rotor speed, w_r; and (c) Mechanical torque, T_m.

VI. Conclusion

In this work, two control strategies for the control of a PMSG for wind energy have been compared and investigated. The models implemented in the simulations include the wind turbine aerodynamics, the PMSG and its FOC control. Variable-speed control has been implemented and compared with two different speed loop control strategies. For the first strategy, standard PI controllers were implemented and the use of pre-filters in these controllers has been analyzed and evaluated.

The second strategy implemented made use of a combination of PI controllers for the inner current loops and a fuzzy controller for the outer speed loop. Simulation results for both control strategies under different wind conditions have been tested and compared. As expected, the fuzzy controller shows better overall operation under varying wind conditions. Moreover, the results show that the fuzzy controller achieved better transient responses under both; large and small disturbances.

The results show that the proposed control structure based on two PI regulators and a fuzzy controller provides an optimal control solution for PMSG wind turbines.

Acknowledgment

This work was supported by the Ministerio de Ciencia y Tecnologia of Spain under Project ENE2007-67033-C03-01 ALT.

References

[1] A. Juamal, D. Venkata, and M. Andrew, “A review of power converter topologies for wind generators”. *Renewable Energy*, 32, pp.2369-2385, 2007.

[2] R. Pena, R. Cardenas, R. Blasco, G. Asher, and J. Clare, “A cage induction generation using back-to-back PWM converters for variable wind speed grid connected wind energy systems”. *In: Proceedings of IEEE IECON’01*, vol. 2, 29 Nov.-2 Dec 2001, pp.1376-1381.

[3] B. Rabelo, and W. Hofmann, “Optimal active and reactive control with the double-fed induction generation in the MW-class wind-turbines”. *In: Proceedings of IEEE fourth international conference on power electronics and drive systems*, vol.1, October 2001, pp.53-58.

[4] I. Schiemenz, and M. Stiebler, “Control of a permanent magnet synchronous generator used in a variable speed wind energy system”. *In: Proceedings of IEEE IEMDC’01*, pp. 872–787.

[5] R.C. Portillo, M.M. Prats, J.I. Leon, J.A. Sanchez, J.M. Carrasco, E. Galvan, and L.G. Franquelo, “Modeling Strategy for Back-to-Back Three-Level Converters Applied to High-Power Wind Turbines”. *IEEE Trans. Ind. Electron*, vol.53, no 5, pp.1483-1491, 2006.

[6] Y.A.-R.I. Mohamed,”Design and implementation of a robust current-control scheme for a PMSM vector drive with a simple adaptive disturbance observer”. *IEEE Trans. Ind. Electron*, vol. 54, no. 4, pp. 1981-1988, Aug. 2007.

[7] S.S. Yang, and Y.S. Zhong, “Robust speed tracking of permanent magnet synchronous motor servo systems by equivalent disturbance attenuation”. *Control Theory & Applications*, IET, vol. 1, no. 3, pp. 595-603, May 2007.

[8] A. Binder, and T. Schneider, “Permanent magnet synchronous generators for regenerative energy conversion - a survey. *European Conference on Power Electronics and Applications EPE 2005*; 11-14 Sep., Dresden, German, pp.1-10.

[9] D. Casadei, F. Profumo, G. Serra, and A. Tani, ”FOC and DTC: Two viable schemes for induction motors torque control,” *IEEE Trans. PowerElectron.*, vol. 17, no. 5, pp. 779-787, Sep. 2002.

[10] A. Murray, M. Palma, and A. Husain, “FOC and DTC: Performance comparison of permanent magnet synchronous motors and controlled induction motors in washing machine applications using sensorless field oriented control. *IEEE Industry Applications Society Annual Meeting 2008*, pp.1-6.

[11] A. Monroy, and L. Alvarez-Icaza, “Real-time identification of wind turbine rotor power coefficient”. *Proceedings of the 45th IEEE Conference on Decision & Control 2006*, pp.369-3695.

[12] Heier, Siegfried. Grid Integration of Wind Energy. John Wiley & Sons Ltd, 1998.

[13] T. Tafticht, K. Agbossou, A. Chérit, and M.L. Doumbia. "Output Power Maximization of a Permanent Magnet Synchronous Generator Based Stand-alone Wind Turbine." IEEE ISIE'06. Motréal, Québec, Canada, 2006, pp. 2412-2416.

[14] D. Fernando, Hernán De Battista, and J. Ricardo. *Wind turbine control systems (Principles, Modelling and Gain Scheduling Design).*Springer 2007.

[15] J. Zaragoza, J. Pou, S. Ceballos, E. Robles, P. Ibañez, and F. Guinjoan, “Control structure with fuzzy supervision of PI parameters in a multilevel converter application”. *IEEE International Symposium on Ind. Electron. Conf.*, ISIE, 2006, pp. 1271 - 1276.

[16] S. Hameed, B. Das, V. Pant, “A self-tuning fuzzy PI controller for TCSC to improve power system stability”. *Electric Power Systems Research*, 78, pp.1726-1735, 2008.

[17] K-M. Passino, and S. Yurkovich. *Fuzzy control*. Addison Wesley Longman, inc. 1998.

[18] T. Takagi, and M. Sugeno, “Fuzzy Identification of systems and its applications to modelling and control. *IEEE Trans. on Systems Man and Cybernetics*, vol. 15, no 1, pp. 116-132. 1958.

[19] F. Iov, A.D. Hansen, P. Sørensen, and F. Blaabjerg. *Wind Turbine Blockset in Matlab/Simulink. Institute of Energy Technology, Aalborg University*. Uni.Print Aalborg University. March 2004.